arXiv:1702.05330v1 [quant-ph] 17 Feb 2017

Arbitrary Nuclear Spin Gates in Diamond Mediated by a NV-center Electron Spin

J. Casanova, Z.-Y. Wang, and M. B. Plenio
Institut für Theoretische Physik and IQST, Albert-Einstein-Allee 11, Universität Ulm, D-89069 Ulm, Germany

We propose a protocol that achieves arbitrary N-qubit interactions between nuclear spins and that can measure directly nuclear many-body correlators by appropriately making the nuclear spins interact with a nitrogen vacancy (NV) center electron spin. The method takes advantage of recently introduced dynamical decoupling techniques and demonstrates that action on the electron spin is sufficient to fully exploit nuclear spins as robust quantum registers. Our protocol is general, being applicable to other nuclear spin based platforms with electronic spin defects acting as mediators as the case of silicon carbide.

Introduction– Nuclear spins in solid-state platforms such as diamond or silicon carbide are natural and reliable quantum registers with exceptional coherence times [1]. In order to realise the potential of this resource for quantum computing [2], quantum simulations [3], and quantum sensing [4, 5], it is necessary to achieve both individual nuclear spin rotations and arbitrary coherent coupling between nuclear spins. In close proximity, nuclear spins exhibit a natural coupling because of their intrinsic nuclear dipolar interactions which may be exploited for quantum simulations [6]. However, this natural coupling is generally small as a consequence of the weak nuclear magnetic moments [3], while the available closest internuclear distances are always lower bounded by the lattice constants of the host material. Furthermore, the spin active nuclear isotopes appear in the platforms of interest with a low natural abundance, e.g. 1.1% and 4.7% for the cases of ^{13}C and ^{29}Si nuclei which are the relevant species for diamond [7, 8] and silicon carbide [9, 10]. Furthermore, the positions of the nuclei are fixed which make the modulation of the internuclear coupling challenging.

The tuning of the direct coupling of nuclear spins is excessively demanding, although it can be suppressed (up to a certain degree) by the application of suitably tuned radio frequency (rf) fields [6, 11, 12]. However, nuclear spins can be coupled to external magnetic fields through Zeeman interactions [13], and more importantly, they can couple to nearby electron spins. In this respect, the electron spin of a NV center is a promising nano-scale device to detect and control nuclear spins using the electron-nuclear hyperfine interaction [7, 8]. The large magnetic moment of electron spins allows a single NV center to couple strongly to many nuclear spins. In addition, with dynamical control achieved due to the application on the NV center of decoupling sequences such as Carr-Purcell-Meiboom-Gill (CPMG) [14, 15], pulse arrangements of the XY kind [16, 17], and adaptive XY sequences [18–20], one can entangle the NV electron to individual nuclear spins (including the ^{14}N nucleus inherent to the NV center) for the sake of electron-nuclear two-qubit quantum gates and quantum algorithms [21–32].

Particularly, the set of techniques developed in [18–20] allow for highly selective and robust electron-nuclear quantum gates evolving according to the Hamiltonians $\sigma_z I_x$ or $\sigma_z I_y$ by using sequences of non-equidistant microwave decoupling pulses. Note that $\sigma_z = |m_s = \pm 1\rangle\langle m_s \pm 1| - |m_s = 0\rangle\langle m_s = 0|$ corresponds to an effective electronic spin-$\frac{1}{2}$ operator [7, 8], while I_x, I_y are nuclear spin operators with $I = \frac{1}{2}$. In addition, in [33] it is shown how the judicious application of a delay window achieves an interaction generated by $\sigma_z I_z$. Furthermore, these techniques can incorporate a decoupling rf field [19, 20, 33] to combine electron-nuclear entangling gate generation with a suppression of the internuclear decoupling.

In this work, we show that arbitrary single, and N-body nuclear spin interactions can be realised easily with an specific combination of electron-nuclear gates. In addition, we demonstrate how the same techniques allow to measure directly nuclear many-body correlators. To exemplify the protocol we use NV centers in diamond as the model system, but our method is general and can be directly exported to other solid-state quantum platforms such as silicon carbide.

Elementary entangling gates– With the techniques in [18–20, 33], one can achieve highly selective entangling quantum gates of the form

$$Q_j^{\alpha}(\varphi) = \exp\left(i\varphi\sigma_z I_j^{\alpha}\right), \tag{1}$$

between the NV electron spin (with Pauli operator σ_z) and the j-th nuclear spin (with the spin operator I_j^{α} and $\alpha = x, y, z$) while prolonging the electron spin coherence. Another important feature is that, as opposed to standard dynamical decoupling methods [14–17], the phase φ is fully tunable. We will see later that this is a crucial requirement for designing our quantum algorithm. In addition, with microwave control, single qubit gates can be applied to the NV electron spin. These are, for instance, $X_{\phi} = e^{i\phi\frac{\sigma_x}{2}}$ i.e. a rotation of an arbitrary and controllable phase ϕ around the x axis although any other direction is available.

Protocol for N-body nuclear interactions– The elementary gates presented before permit the implementation of N-body interactions (denoted in the following by U_{ϕ}) between the nuclear spins that can be individually addressed by the NV center. For example, having the entangling gates $Q_{j_1}^{\alpha_1}(\varphi_1)Q_{j_2}^{\alpha_2}(\varphi_2)$ at hand, one can demonstrate the following equality (up to an irrelevant global phase):

$$\begin{aligned} U_{\phi} &= Q_{j_1}^{\alpha_1}(\varphi_1)Q_{j_2}^{\alpha_2}(\varphi_2)X_{2\phi+\pi}Q_{j_1}^{\alpha_1}(\varphi_1)Q_{j_2}^{\alpha_2}(\varphi_2)X_{\pi} \\ &= e^{i\phi\sigma_x(\cos\varphi_1 - 2i\sin\varphi_1\sigma_z I_{j_1}^{\alpha_1})(\cos\varphi_2 - 2i\sin\varphi_2\sigma_z I_{j_2}^{\alpha_2})}, \end{aligned} \tag{2}$$

which contains two-qubit, and many-body (in this specific

case three-body) interactions involving the electron and the nuclear spins.

We want to note that an especially interesting situation is realised when $\varphi_1 = \varphi_2 = \frac{\pi}{2}$, i.e. when we are making interact with the same phase the electron spin with different nuclei. In this case we have $U_\phi = \exp\left[-i4\phi\sigma_x I_{j_1}^{\alpha_1} I_{j_2}^{\alpha_2}\right]$ namely a three-body time evolution operator where the phase ϕ corresponds to the one of the central gate, $X_{2\phi+\pi}$, on the first line in Eq. (2).

Now it is possible to generalise the results in Eq. (2) and demonstrate that with the following sequence of gates

$$U_\phi \;=\; Q_N X_{2\phi+\pi} Q_N X_\pi, \tag{3}$$

where $Q_N = \prod_{n=1}^{N} Q_{j_n}^{\alpha_n}(\varphi_n)$, N labels the total number of addressable nuclear spins, $\alpha_n = x, y, z$, and by noting that $[Q_{j_n}^{\alpha_n}(\varphi_n), Q_{j_m}^{\alpha_m}(\varphi_m)] = 0$ for $n \neq m$, i.e. the different entangling gates commute, one can find that for $\varphi_n = \frac{\pi}{2}\ \forall n$, and in the case $N = 2M$ (i.e. we are subsequently addressing an even number of nuclear spins) the time evolution operator is

$$U_\phi^e \;=\; \exp\left[(-1)^M i\, 2^{2M}\phi\ \sigma_x \prod_{n=1}^{2M} I_{j_n}^{\alpha_n}\right]. \tag{4}$$

In the same manner, for $N = 2M+1$ (an odd number of nuclear spins are addressed) we have

$$U_\phi^o \;=\; \exp\left[(-1)^{(M+1)} i\, 2^{2M+1}\phi\ \sigma_y \prod_{n=1}^{2M+1} I_{j_n}^{\alpha_n}\right]. \tag{5}$$

Note that in both cases we have a $(N+1)$-body evolution that involves the electron and nuclear spins.

Now, if the U_ϕ^e or U_ϕ^o operators act on an initial state such that, for the even case, we have $\rho_{t=0}^e = |x_\pm\rangle\langle x_\pm| \otimes \rho_N$ where $\sigma_x|x_\pm\rangle = \pm|x_\pm\rangle$, while the odd initial state is $\rho_{t=0}^o = |y_\pm\rangle\langle y_\pm| \otimes \rho_N$ with $\sigma_y|y_\pm\rangle = \pm|y_\pm\rangle$ and ρ_N represents an initial nuclear state, we have the following two possibilities

$$U_\phi^e\, \rho_{t=0}^e (U_\phi^e)^\dagger = |x_\pm\rangle\langle x_\pm| \otimes \tilde{U}_{\pm\phi}^e\, \rho_N\, (\tilde{U}_{\pm\phi}^e)^\dagger \tag{6}$$

and

$$U_\phi^o\, \rho_{t=0}^o (U_\phi^o)^\dagger = |y_\pm\rangle\langle y_\pm| \otimes \tilde{U}_{\pm\phi}^o\, \rho_N\, (\tilde{U}_{\pm\phi}^o)^\dagger, \tag{7}$$

where the N-body nuclear operators $\tilde{U}_{\pm\phi}^e$, $\tilde{U}_{\pm\phi}^o$ read

$$\tilde{U}_{\pm\phi}^e = \exp\left[-(1)^M i\, 2^{2M}(\pm\phi) \prod_{n=1}^{2M} I_{j_n}^{\alpha_n}\right], \tag{8}$$

and

$$\tilde{U}_{\pm\phi}^o = \exp\left[-(1)^{(M+1)} i\, 2^{2M+1}(\pm\phi) \prod_{n=1}^{2M+1} I_{j_n}^{\alpha_n}\right]. \tag{9}$$

It is also important to note that the gates $X_{2\phi+\pi}$ and X_π in Eq. (3) can be replaced by $Y_{2\phi+\pi}$ and Y_π where $Y_\phi = e^{i\phi\frac{\sigma_y}{2}}$, or for any other gate that implies a rotation on the XY plane, which would give rise to a set of results similar to the ones in Eqs. (4), (5), (8), and (9).

In this manner we have realised an effective N-body interaction acting on a set of nuclei, while the electron spin gets uncoupled after the processes. We would like to note that Eqs. (8) and (9) allows one to couple distant nuclear spins and, remarkably, the achieved phase ϕ can be easily extended without affecting significantly to the total time of the protocol. In this respect note that ϕ is introduced through a single-qubit gate on the electron spin that can be implemented in a time on the order of nanoseconds. Furthermore, an electron spin rotation to change $|x_\pm\rangle \to |y_\pm\rangle$ allows us to subsequently combine the final results in Eqs. (8), (9) in order to concatenate a set of N-qubit quantum gates on different nuclei.

In the same manner, and using again the NV center spin as the interaction mediator, a single entangling gate $Q_{j_n}^{\alpha_n}(\varphi_n)$ can be used to individually rotate any addressable spin by an arbitrary phase. This is achieved by simply noting that

$$Q_{j_n}^{\alpha_n}(\varphi_n)|z_\pm\rangle\langle z_\pm| \otimes \rho_N (Q_{j_n}^{\alpha_n})^\dagger = |z_\pm\rangle\langle z_\pm| \otimes e^{\pm\left(i\varphi_n I_{j_n}^{\alpha_n}\right)} \rho_N e^{\mp\left(i\varphi_n I_{j_n}^{\alpha_n}\right)}, \tag{10}$$

where $\sigma_z|\pm z\rangle = \pm|\pm z\rangle$. Hence, single nuclear spin rotations can be applied without having to introduce weak control rf fields that would require further calibration of the system.

In the end of the computing processes a selective SWAP gate between the electron and a target nuclear spin allows to transfer the nuclear spin quantum state to the NV center and reconstruct the nuclear spin state, or measure a nuclear spin operator, by optical readout applied on the NV center which, at low temperatures, can achieve fidelities exceeding 95% [32]. In this respect, we want to note that a SWAP gate can be performed, up to a global phase, as $\mathrm{SWAP}_{e,j_n} = \exp\left[i\frac{\pi}{2}(\sigma_z I_{j_n}^z + \sigma_x I_{j_n}^x + \sigma_y I_{j_n}^y)\right] = \exp\left[i\frac{\pi}{2}\sigma_z I_{j_n}^z\right] \exp\left[i\frac{\pi}{2}\sigma_x I_{j_n}^x\right] \exp\left[i\frac{\pi}{2}\sigma_y I_{j_n}^y\right]$, where each of the previous two-qubit gates can be realised with [18–20, 33] plus additional single-qubit gates on the electron spin. Note also that a selective iSWAP gate (with $\mathrm{iSWAP}_{e,j_n} = \exp\left[i\frac{\pi}{2}(\sigma_x I_{j_n}^x + \sigma_y I_{j_n}^y)\right] = \exp\left[i\frac{\pi}{2}\sigma_x I_{j_n}^x\right] \exp\left[i\frac{\pi}{2}\sigma_y I_{j_n}^y\right]$) is also valid to retrieve the nuclear state information.

Measuring nuclear many-body correlations– The same techniques can be applied to directly measure the expectation value of delocalised N-body nuclear operators. This can be done through the next equality (for the sake of simplicity we develop here the case for U_ϕ^e while the odd case, i.e. the case for U_ϕ^o, is similar). After a set of N-body operations we have that the final state is $\rho = \rho_e \otimes \rho_n(t)$, with $\rho_e = |\alpha_\pm\rangle\langle\alpha_\pm|$ and $\alpha = x, y$ or z depending on the sequence of gates we performed. Now we can take, with an electron spin flip, the state ρ_e to an eigenstate of σ_z i.e. $\rho_e \to |1\rangle\langle 1|$ with $\sigma_z|1\rangle = |1\rangle$, apply an additional gate U_ϕ^e and measure, for example, the σ_y electronic operator. This process leads to

$$\begin{aligned}\langle\sigma_y\rangle \;&=\; \mathrm{Tr}\Big[\rho_e \otimes \rho_n(t)(U_\phi^e)^\dagger \sigma_y U_\phi^e\Big] \\ &=\; \mathrm{Tr}\Big[\rho_e \otimes \rho_n(t)\, e^{\left[(-1)^M(-i)\ 2^{2M}(2\phi)\ \sigma_x \prod_{n=1}^{2M} I_{j_n}^{\alpha_n}\right]}\ \sigma_y\Big].\end{aligned} \tag{11}$$

Now, if we select the phase ϕ such that $(-1)^M 2\phi = (\frac{\pi}{2} + m\,2\pi)$ with $m \in \mathbb{Z}$, we find that $\langle\sigma_y\rangle = \mathrm{Tr}\Big[\rho_e \otimes \rho_n(t)\ \sigma_z \prod_{n=1}^{2M} \sigma_{j_n}^{\alpha_n}\Big]$ and one can write

$$\langle\sigma_y\rangle = \mathrm{Tr}_n\Big[\rho_n(t) \prod_{n=1}^{2M} \sigma_{j_n}^{\alpha_n}\Big] = \Big\langle \prod_{n=1}^{2M} \sigma_{j_n}^{\alpha_n}\Big\rangle, \tag{12}$$

where $\mathrm{Tr}_n[\,\cdot\,]$ denotes the trace over the nuclear degrees of freedom. In this manner a highly delocalised nuclear operator gets encoded into an easy to measure electronic expectation value.

Implementation with NV centers– In order to demonstrate the working principle of our protocol we will consider diamond technologies, i.e. a NV center in the presence of a nuclear spin bath, as the target system to numerically study our method. When a strong magnetic field B_z is aligned with the NV axis, the $\hat{z}$ direction, the Hamiltonian of the coupled system in the rotating frame of the free energy electronic spin Hamiltonian $H_0 = DS_z^2 - \gamma_e B_z S_z$ reads ($\hbar = 1$)

$$H = A^{\parallel} S_z - \sum_j \gamma_j B_z I_j^z + S_z \sum_j \vec{A}_j \cdot \vec{I}_j + H_c. \tag{13}$$

Here, the first term $A^{\parallel} S_z$ with $A^{\parallel} \approx -(2\pi) \times 2.162$ MHz, see [34], and the spin-1 operator $S_z = |1\rangle\langle 1| - |-1\rangle\langle -1|$, corresponds to the longitudinal component of the coupling with the ^{14}N nucleus adjacent to the vacancy. In our simulations, instead of using the ^{14}N nucleus as a resource qubit, we take it as the origin of a large detuning error with magnitude $|A^{\parallel}|$ [35] for demonstrating the robustness of our protocol. However if the ^{14}N is polarised at the beginning of the operational processes that detuning is negligible. The constants $\gamma_e = -(2\pi) \times 2.8024\ \frac{\mathrm{MHz}}{\mathrm{G}}$ and $\gamma_j \equiv \gamma_{^{13}\mathrm{C}} = (2\pi) \times 1.0705\ \frac{\mathrm{kHz}}{\mathrm{G}}$ $\forall\, j$ represent the electronic and nuclear (in this case for the ^{13}C nucleus) gyromagnetic ratios.

The interaction between the NV center and the nuclear spins is mediated by the hyperfine vector that we will consider as dipolar like, i.e. $\vec{A}_j = \frac{\mu_0 \gamma_e \gamma_j}{4\pi |\vec{r}_j|^3}[\hat{z} - 3\frac{(\hat{z}\cdot\vec{r}_j)\vec{r}_j}{|\vec{r}_j|^2}]$, where $\vec{r}_j$ is the vector that connects the NV center and each environmental nuclei. Note also that, because of recently developed positioning methods [19] we will take $\vec{A}_j$ as known quantities. The large zero field splitting $D = (2\pi) \times 2.87$ GHz had allowed us to neglect non-secular components in Eq. (13). Furthermore, an external microwave control can be introduced in Eq. (13) through the term $H_c = \Omega(|1\rangle\langle 0|e^{i\vartheta} + |0\rangle\langle 1|e^{-i\vartheta})$ with Ω being the Rabi frequency of the microwave field. In this manner, we are selecting the electronic spin subspace $|0\rangle$, $|1\rangle$ to define our qubit. In our numerics we will additionally introduce an error in Ω for considering realistic experimental conditions. More specifically, if the required time for a π-flip rotation of the electron spin is $t_\pi = \frac{1}{4\Omega}$, we will effectively introduce a Rabi frequency $\Omega(1+\epsilon)$ with ϵ the relative error that we will set as 1% [36]. Finally ϑ is a phase that, for the sake of robustness, remains constant during each microwave pulse but change between pulses [18, 37, 38].

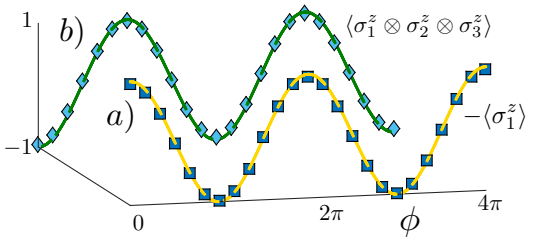

FIG. 1: Expectation value of a) the σ_1^z operator. Solid line, ideal result according to the propagator in the second line of Eq. (15) while the squares correspond to the result when the sequence of gates in the first line of Eq. (15) is applied. b) Expectation value of the delocalised operator $\sigma_1^z \otimes \sigma_2^z \otimes \sigma_3^z$. The solid line represents the ideal evolution while diamonds are the result of applying our method. All the points in the plot (squares and diamonds) correspond to the application of 3202 microwave pulses with a π pulse time of 12.5 ns, and a total evolution time of ≈ 0.7 ms to generate the propagator in Eq. (15). Note that this value is independent of the achieved phase ϕ.

Hence, under the action of the microwave control pulses the final Hamiltonian is

$$H = -\sum_j \omega_j\, \hat{\omega}_j \cdot \vec{I}_j + F(t)\, \sigma_z \sum_j \vec{A}_j \cdot \vec{I}_j, \tag{14}$$

where $\sigma_z = |1\rangle\langle 1| - |0\rangle\langle 0|$, $F(t) = \pm 1$ is the modulation function appearing because of the action of π-pulses upon the electron spin, and $\vec{\omega}_j = \gamma_{^{13}\mathrm{C}} B_z \hat{z} - \frac{1}{2}\vec{A}_j$ with $\omega_j = |\vec{\omega}_j|$ and $\hat{\omega}_j = \vec{\omega}_j/|\vec{\omega}_j|$. In this ideal description the detuning term $A^{\parallel} S_z$ has been eliminated because of the external microwave driving, however our numerics will incorporate it since they are performed assuming Eq. (13) as the starting point. In addition, we will not consider electron relaxation processes because, at low temperatures around 4 K, measurements of the relaxation time (T_1) on the order of several seconds have already been reported [31, 39] which largely exceeds the time for performing entangling nuclear gates.

Numerical results– We have numerically simulated the three-body nuclear time evolution operator $\exp(i2^3\phi\, I_x^1 I_x^2 I_x^3)$, that gives rise to maximally entangled GHZ like states [40] when the nuclear register is initialized into the state $|\downarrow\downarrow\downarrow\rangle$. The latter can be prepared by polarisation transfer from the electron spin, see for example [29–31], or by dynamical nuclear polarisation (DNP) [41–43]. The three-body nuclear propagator can be achieved by applying the sequence in Eq. (3) with $Q_N = \prod_{n=1}^{3} Q_{j_n}^{\alpha_n}(\varphi_n)$ where $\alpha_1 = \alpha_2 = \alpha_3 = x$. More specifically, this is

$$\begin{aligned} U_\phi &= Q_1^x(\varphi_1) Q_2^x(\varphi_2) Q_3^x(\varphi_3) X_{2\phi+\pi} Q_1^x(\varphi_1) Q_2^x(\varphi_2) Q_3^x(\varphi_3) X_\pi \\ &= -\exp\Big(i2^3\phi\ \sigma_y I_1^x I_2^x I_3^x\Big) = -\exp\Big(i\phi\ \sigma_y \sigma_1^x \sigma_2^x \sigma_3^x\Big). \end{aligned} \tag{15}$$

We selected a three qubit nuclear register such that $\vec{A}_1 = (2\pi) \times (-56, -32, -45)$ kHz, $\vec{A}_2 = (2\pi) \times (-7.6, 39, 52)$ kHz, $\vec{A}_3 = (2\pi) \times (-22, 13, 96)$ kHz, all of them corresponding to nuclei located in available positions of the diamond lattice, and the static magnetic field is $B_z = 0.65$ T. Furthermore,

and although not included in our theoretical description in Eqs. (13) and (14), we have also taken into account in the numerics the effect of internuclear interactions. These produce a coupling between the i-th and j-th nuclei of the form $g_{i,j} = \frac{\hbar\mu_0\gamma^2_{^{13}\mathrm{C}}}{2d^3_{i,j}}[1-3(n^z_{i,j})^2]$ with $d_{i,j}$ the relative distance between nuclei and $n^z_{i,j}$ the normalized $\hat{z}$ component of their relative positioning vector. In our case we have $g_{1,2} \approx -(2\pi) \times 20$ Hz, $g_{1,3} \approx -(2\pi) \times 10$ Hz, and $g_{2,3} \approx (2\pi) \times 7.5$ Hz. Figure 1 shows the evolution of the expectation value of a single nucleus σ^z_1 and of the delocalised operator $\sigma^z_1 \otimes \sigma^z_2 \otimes \sigma^z_3$. The solid line corresponds to the ideal behavior while squares and diamonds represent the result when our method is applied. Furthermore, we computed that the fidelity for the creation of a three-qubit GHZ-like nuclear state of the form $|\Psi\rangle = \exp(i\frac{\pi}{4}\sigma_y\sigma^x_1\sigma^x_2\sigma^x_3)|y_+\rangle|\downarrow\downarrow\downarrow\rangle = |y_+\rangle\frac{1}{\sqrt{2}}(|\downarrow\downarrow\downarrow\rangle + i|\uparrow\uparrow\uparrow\rangle)$ is 98.8%. This state has been prepared employing the same number of imperfect pulses, 3202, than the one used for Fig 1.

Further applications– The generation of these kind of gates, single- and N-qubit, allows to deal with problems involving fermionic interactions. It is known that any creation or annihilation fermionic operator admits a form in terms of tensorial products of Pauli matrices when the Jordan-Wigner transformation is applied [44]. Hence, an appropriate application of our techniques would be of benefit to implement dynamics that include interacting fermions, e.g. quantum chemistry problems, in a solid-state quantum platform. Furthermore, the access to arbitrary multi-qubit spin propagators is of interest for simulating spin models with topological order [45], as well as to generate dynamics and to perform measurements in different models of quantum computing as the case of deterministic quantum computation with one quantum bit, the DQC1 protocol, that do not require to initially polarise the nuclear register [46, 47].

Conclusion– We presented a protocol that allows the generation of single and N-qubit quantum gates between nuclear spins in a solid state register such as diamond, as well as to measure highly delocalised nuclear spin correlators. These gates are mediated by an effective electron spin, for example a NV center, that can be externally controlled with microwave radiation. The method is general and, therefore, applicable to other lattice defects as silicon carbide or germanium vacancy centers.

Acknowledgements– The authors acknowledge J. F. Haase, T. Theurer, and R. Puebla for their useful comments on the manuscript. This work was supported by the Alexander von Humboldt Foundation, the ERC Synergy grant BioQ, the EU projects DIADEMS, EQUAM and HYPERDIAMOND as well as the DFG via the SFB TRR/21 and the SPP 1601. J. C. acknowledges Universität Ulm for a Forschunsgbonus.

[1] P. C. Maurer, G. Kucsko, C. Latta, L. Jiang, N. Y. Yao, S. D. Bennett, F. Pastawski, D. Hunger, N. Chisholm, M. Markham, D. J. Twitchen, J. I. Cirac, and M. D. Lukin, Science **336**, 1283 (2012).

[2] M. A. Nielsen and I. L. Chuang, *Quantum Computation and Quantum Information* (Cambridge University press, Cambridge, 2000).

[3] I. M. Georgescu, S. Ashhab, and Franco Nori, Rev. Mod. Phys. **86**, 153 (2014).

[4] C. L. Degen, F. Reinhard, and P. Cappellaro, arXiv: 1611.02427.

[5] Y. Wu, F. Jelezko, M. B. Plenio, and T. Weil, Angew. Chem. Int. Ed. **55**, 6586 (2016).

[6] J. Cai, A. Retzker, F. Jelezko, and Martin B. Plenio, Nat. Phys. **9**, 168 (2013).

[7] M. W. Doherty, N. B. Manson, P. Delaney, F. Jelezko, J. Wrachtrup, and L. C. L. Hollenberg, Phys. Reports **528**, 1 (2013).

[8] V.V. Dobrovitski, G.D. Fuchs, A.L. Falk, C. Santori, and D.D. Awschalom, Annu. Rev. Condens. Matter Phys **4**, 23 (2013).

[9] P. G. Baranov, I. V. Il´in, E. N. Mokhov, M. V. Muzafarova, S. B. Orlinskii and J. Schmidt, JETP Lett. **82**, 441 (2005).

[10] H. Seo, A. L. Falk, P. V. Klimov, K. C. Miao, G. Galli, and D. D. Awschalom, Nat. Commun. **7** 12935 (2016).

[11] M. Lee and W. I. Goldburg, Phys. Rev. **140**, A1261 (1965).

[12] C. A. Michal, S. P. Hastings, and L. H. Lee, J. Chem. Phys. **128**, 052301 (2008).

[13] A. Abragam, *The Principles of Nuclear Magnetism* (Oxford University Press, London, 1961).

[14] H. Y. Carr and E. M. Purcell, Phys. Rev. **94**, 630 (1954).

[15] S. Meiboom and D. Gill, Rev. Sci. Instrum. **29**, 688 (1958).

[16] A. A. Maudsley, J. Magn. Reson. **69**, 488 (1986).

[17] T. Gullion, D. B. Baker, and M. S. Conradi, J. Magn. Reson. **89**, 479 (1990).

[18] J. Casanova, Z. -Y. Wang, J. F. Haase, and M. B. Plenio, Phys. Rev. A **92**, 042304 (2015).

[19] Z. -Y. Wang, J. F. Haase, J. Casanova, and M. B. Plenio, Phys. Rev. B **93**, 174104 (2016).

[20] J. Casanova, Z. -Y. Wang, and M. B. Plenio, Phys. Rev. Lett. **117**, 130502 (2016).

[21] M. V. Gurudev Dutt, L. Childress, L. Jiang, E. Togan, J. Maze, F. Jelezko, A. S. Zibrov, P. R. Hemmer, and M. D. Lukin, Science **316**, 1312 (2007).

[22] P. Neumann, J. Beck, M. Steiner, F. Rempp, H. Fedder, P. R. Hemmer, J. Wrachtrup, and F. Jelezko, Science **329**, 542 (2010).

[23] L. Robledo, L. Childress, H. Bernien, B. Hensen, P. F. A. Alkemade, and R. Hanson, Nature **477**, 574 (2011).

[24] T. van der Sar, Z. H. Wang, M. S. Blok, H. Bernien, T. H. Taminiau, D. M. Toyli, D. A. Lidar, D. D. Awschalom, R. Hanson, and V. V. Dobrovitski, Nature **484**, 82 (2012).

[25] S. Kolkowitz, Q. P. Unterreithmeier, S. D. Bennett, and M. D. Lukin, Phys. Rev. Lett. **109**, 137601 (2012).

[26] T. H. Taminiau, J. J. T. Wagenaar, T. van der Sar, F. Jelezko, V. V. Dobrovitski, and R. Hanson, Phys. Rev. Lett. **109**, 137602 (2012).

[27] N. Zhao, J. Honert, B. Schmid, M. Klas, J. Isoya, M. Markham, D. Twitchen, F. Jelezko, R.-B. Liu, H. Fedder, and J. Wrachtrup, Nature Nanotechnology **7** 657 (2012).

[28] G.-Q. Liu, H. C. Po, J. Du, R.-B. Liu, and X.-Y. Pan, Nat. Comm. **4**, 2254 (2013).

[29] T. H. Taminiau, J. Cramer, T. van der Sar, V. V. Dobrovitski, and R. Hanson, Nature Nanotech. **9**, 171 (2014).

[30] G. Waldherr, Y. Wang, S. Zaiser, M. Jamali, T. Schulte-Herbrüggen, H. Abe, T. Ohshima, J. Isoya, J.F. Du, P. Neumann, and J. Wrachtrup, Nature **506**, 204 (2014).

[31] J. Cramer, N. Kalb, M. A. Rol, B. Hensen, M. S. Blok, M. Markham, D. J. Twitchen, R. Hanson, and T. H. Taminiau, Nat. Commun. **7**, 11526 (2016).

[32] B. Hensen, H. Bernien, A.E. Dréau, A. Reiserer, N. Kalb, M.S. Blok, J. Ruitenberg, R.F.L. Vermeulen, R.N. Schouten, C. Abellán, W. Amaya, V. Pruneri, M. W. Mitchell, M. Markham, D.J. Twitchen, D. Elkouss, S. Wehner, T.H. Taminiau, and R. Hanson, Nature **526**, 682 (2015).

[33] Z. -Y. Wang, J. Casanova, and M. B. Plenio, arXiv:1604.05731.

[34] M. Chen, M. Hirose, and P. Cappellaro, Phys. Rev. B **92** 020101(R) (2015).

[35] M. Loretz, J. M. Boss, T. Rosskopf, H. J. Mamin, D. Rugar, and C. L. Degen, Phys. Rev. X **15**, 021009 (2015).

[36] J.-M. Cai, B. Naydenov, R. Pfeiffer, L. P. McGuinness, K. D. Jahnke, F. Jelezko, M. B. Plenio, and A. Retzker, New. J. Phys. **14**, 113023 (2012).

[37] C. A. Ryan, J. S. Hodges, and D. G. Cory, Phys. Rev. Lett. **105**, 200402 (2010).

[38] A. M. Souza, G. A. Alvarez, and D. Suter, Phys. Rev. Lett. **106**, 240501 (2011).

[39] A. Jarmola, V. M. Acosta, K. Jensen, S. Chemerisov, and D. Budker, Phys. Rev. Lett. **108**, 197601 (2012).

[40] D. M. Greenberger, M. Horne, and A. Zeilinger, *Bell´s Theorem, Quantum Theory, and Conceptions of the Universe*, edited by M. Kafatos Kluwer, Dordrecht, 1989 , p. 69.

[41] P. London, J. Scheuer, J.-M. Cai, I. Schwarz, A. Retzker, M. B. Plenio, M. Katagiri, T. Teraji, S. Koizumi, J. Isoya, R. Fischer, L. P. McGuinness, B. Naydenov, and F. Jelezko, Phys. Rev. Lett. **111**, 067601 (2013).

[42] Q. Chen, I. Schwarz, F. Jelezko, and M. B. Plenio, Phys. Rev. B **92**, 184420 (2015).

[43] J. Scheuer, I. Schwartz, Q. Chen, D. Schulze-Sünninghausen, P. Carl, P. Höfer, A. Retzker, H. Sumiya, J. Isoya, B. Luy, M. B. Plenio, B. Naydenov, and F. Jelezko, New. J. Phys. **18**, 013040 (2016).

[44] P. Jordan and E. Wigner, Z. Phys. **47**, 631 (1928).

[45] C. Nayak, S. H. Simon, A. Stern, M. Freedman, S. Das Sarma, Rev. Mod. Phys. **80**, 1083 (2008).

[46] S. Parker and M. B. Plenio, J. Mod. Opt. **49**, 1325 (2002).

[47] S. Boixo and R. D. Somma, Phys. Rev. A **77**, 052320 (2008).